EUROX 15 (2022) 100153

Contents lists available at ScienceDirect

European Journal of Obstetrics & Gynecology and Reproductive Biology: X

journal homepage: www.journals.elsevier.com/european-journal-of-obstetrics-and-gynecology-and-reproductive-biology

# Histopathological features in advanced abdominal pregnancies co-infected with SARS-CoV-2 and HIV-1 infections: A case evaluation

S. Ramphal [a,*], N. Govender [b], S. Singh [c], OP Khaliq [d], T. Naicker [c]

[a] Department of Obstetrics and Gynaecology, School of Clinical Medicine, College of Health Sciences, University of KwaZulu-Natal, Durban, South Africa
[b] Department of Basic Medical Sciences, Durban University of Technology, Durban, KwaZulu-Natal, South Africa
[c] Optics and Imaging Centre, Doris Duke Medical Research Institute, College of Health Sciences, University of KwaZulu-Natal, Durban, South Africa
[d] Department of Paediatrics and Child Health, School of Clinical Medicine, Faculty of Health Sciences, University of the Free State, Bloemfontein, South Africa

ARTICLE INFO

*Keywords:*
Advanced abdominal pregnancy
SARS-CoV-2
HIV infection
Placenta
Urological pathology

ABSTRACT

*Objectives:* This study aims to provide a semi-qualitative histopathological report of the dual SARS-CoV-2 and HIV infected placentae in the third trimester of Advanced Abdominal Pregnancy (AAP).
*Study design:* Four AAP placentae in the third trimester of pregnancy (two positive for HIV-1 and two positives for SARS-CoV-2) were histologically examined.
*Results:* The SARS-CoV-2$^{+}$ HIV$^{+}$ placentae were dysmorphic in shape compared to the flattened disc-like shape noted in the SARS-CoV-2$^{+}$HIV$^{-}$, SARS-CoV-2$^{-}$HIV$^{+}$and SARS-CoV-2$^{-}$HIV$^{-}$ placentae. Diffused syncytial knots and syncytial degeneration were observed in all placentae. Intermittent cytotrophoblast increase, perivillous and intravillous fibrin deposition, mononuclear inflammatory cells with widespread degeneration/necrosis of the syncytiotrophoblast and microcalcification were pronounced in the SARS-CoV-2$^{+}$HIV$^{+}$ compared to the SARS-CoV-2$^{+}$HIV$^{-}$ placentae. Vascular pathological changes included thrombi, ectasis, mural hypertrophy and atherotic vessels.
*Conclusion:* Elevated syncytial trophoblast injury, villitis, microcalcifications and mineralisation of the syncytial basement membrane in the AAP placentae may be due to SARS-CoV-2 viral transgression instead of HIV infection alone. Vascular malperfusion is suggestive of a hypoxic insult arising from a compensatory response to meet the fetal oxygen and nutrient demands of an AAP. Placentae from HIV infected women on antiretroviral treatment were characterised by vascular malperfusion.

## Introduction

The province of KwaZulu-Natal, South Africa (SA) is considered the epicentre of the HIV pandemic where one in three pregnant women attending antenatal clinics are HIV infected [1,2]. Human Immunodeficiency Virus infection in pregnancy increases the risk of maternal and perinatal morbidity and mortality [3]. Recently, the COVID-19 pandemic has been reported to increase the maternal mortality ratio in SA by 30% [4]. Similarly, a large multinational cohort study across 18 countries has demonstrated that COVID-19 in pregnancy is associated with increase in maternal and neonatal morbidity and mortality [5].

Advanced abdominal pregnancy (AAP) refers to a pregnancy that develops in the abdominal cavity and proceeds beyond 20 weeks of gestation [6,7] and it is rare for these pregnancies to reach the third trimester with a healthy viable foetus [8]. To-date, management of the placenta at delivery is controversial. Ligation of the umbilical cord and leaving the placenta in situ is preferred by most surgeons because of the risk of maternal haemorrhage following placental removal. It is therefore not surprising that there is limited information on the histological evaluation of AAP placentae.

Histopathologic examination of placental tissue mimics a window to the health of both mother and baby. There is however a paucity of information on placental histology of AAP with viral infections. Hence, in the face of HIV and COVID-19 infections, we report on placental histopathology of four rare cases of AAP with live births.

* Correspondence to: Department of Obstetrics and Gynaecology, Nelson Mandela Medical School, University of KwaZulu-Natal, Durban, South Africa.
*E-mail address:* RAMPHALS1@ukzn.ac.za (S. Ramphal).

https://doi.org/10.1016/j.eurox.2022.100153
Received 27 January 2022; Received in revised form 27 April 2022; Accepted 11 May 2022
Available online 14 May 2022

## Material and methods

### *Ethics approval*

This study was conducted at a tertiary hospital in SA. Participants were referred from surrounding healthcare facilities for specialist care. Institutional ethical approval (BE026/010), regulatory health authority permission and informed consent were obtained prior to collection of placental samples.

### *Study population*

The placentae were obtained from four women who had scheduled laparotomy to deliver the AAP with live foetuses in the third trimester of pregnancy. Of the four placentae, two were SARS-CoV-2 positive and two were SARS-CoV-2 negative women. The placentae were further stratified by the participants HIV status into SARS-CoV-$2^+$ $HIV^+$; SARS-CoV-$2^+$ $HIV^-$; SARS-CoV-$2^-$ $HIV^+$ and SARS-CoV-$2^-$ $HIV^-$ sub-groups. The diagnosis of SARS-CoV-2 was confirmed with polymerase chain testing.

### *Placental handling during surgical removal*

Laparotomy were performed through a midline abdominal incision. The placental location and findings at laparotomy are shown in Table 1. In all the cases, the omentum and bowel were closely adherent to the amniotic sac. The foetus was delivered after opening the amniotic sac furthest away from the placental attachment, at the least vascular site. Following delivery of the foetus, the umbilical cord was ligated, and a careful inspection was performed to identify the vascular supply to the placenta. The placenta was subsequently carefully mobilized, with the omentum and bowel separated from the sac. A systematic approach using surgical clamps and ties with ligation of the feeding vessels was performed. In all the cases, the infundibular pelvic and omental vessels were the main vascular supply. The placenta was removed "enbloc" and immediately stored in formalin for histopathological analyses. Placental weights were only available for the SARS-CoV-$2^+$ infected placentae.

### *Histological placental preparation*

Placental samples (central region) were fixed in 10% buffered formaldehyde, dehydrated, infiltrated and embedded into paraffin wax blocks as per standard laboratory procedure [9]. Sections of placental tissue (3 μm) were de-paraffinized, rehydrated for haematoxylin and eosin staining, dehydrated and "cover-slipped" as previously reported [10]. Sections were then examined using the ZEISS Axio Imager 2 and images were captured using the Zen (Blue edition) software (Cariss-Strasse, Oberkochen, Germany).

## Results

The demographic and clinical data for all four groups are shown in Table 2. All participants were in their 3rd trimester of pregnancy, and one patient had a history of a previous ectopic pregnancy. None of the study patients had evidence of urinary tract infections or proteinuria.

**Table 2**
Clinical Characteristics and Laboratory Data of the Advanced Abdominal Pregnancies and their Babies.

| Clinical Parameters | SARS-CoV-$2^+$ $HIV^+$ | SARS-CoV-$2^+$ $HIV^-$ | SARS-CoV-$2^-$ $HIV^+$ | SARS-CoV-$2^-$ $HIV^-$ |
|---|---|---|---|---|
| Maternal age (years) | 36 | 21 | 39 | 29 |
| Parity | 0 | 0 + (1 Ectopic) | 3 | 2 |
| Gravidity | 1 | 2 | 4 | 3 |
| Blood Pressure (mmHg) | 110/53 | 101/62 | 100/60 | 120/70 |
| Gestational age (weeks) | 34 | 37 | 36 | 30 |
| Hemoglobin (g/dl) | 13.8 | 13.3 | 11.1 | 10.3 |
| Viral load (cells/ μL) | LTDL (FDC) | – | LTDL (FDC) | – |
| CD4 count (cells/μL) | 500 | – | 484 | – |
| TB screening | Negative | Negative | Negative | Negative |
| COVID screening | Positive (27 weeks) | Positive (34 weeks) | Negative | Negative |
| Rapid Plasma Reagin | Negative | Negative | Negative | Negative |
| Rhesus Grouping | Positive | Positive | Positive | Positive |
| Baby weight (kg) | 1.98 | 2.95 | 2.78 | 1.2 |
| Fetal abnormality | dysmorphic features with left foot abnormality | nil | nil | nil |

LTDL: lower than detectable load; FDC: fixed dose combination

Blood pressure levels were normal in all participants, with no clinical, X-Ray or laboratory evidence of TB and syphilis co-infections. Also, two women were SARS-CoV-2 positive (one $HIV^+$ and one $HIV^-$) on PCR testing whilst two were SARS-CoV-2 negative (one $HIV^+$ and one $HIV^-$). Both SARS-CoV-2 positive patients were asymptomatic, diagnosed in the third trimester and delivery effected greater than 14 days from diagnosis. All babies at birth were alive, did not require neonatal intensive care and were alive at the time of hospital discharge.

## Placental findings

### *Gross morphological features*

Macroscopically, the SARS-CoV-$2^+$ $HIV^+$ placentae was dysmorphic in appearance (Fig. 1a; approximately 811 g) vs the SARS-CoV-$2^+$ $HIV^-$ placenta (Fig. 1b, 677 g). In contrast, the SARS-CoV-$2^-$ $HIV^-$ and SARS-CoV-$2^-$ $HIV^+$ placentae were disc like in appearance. There was no evidence of infarcts. Apart from the umbilical cord insertion, differentiation between foetal (chorionic plate) and maternal portion (basal plate decidua) was difficult. The insertion sites of the umbilical cord were eccentric across all placentae.

**Table 1**
Placental and Fetal Findings at Laparotomy.

| Findings at surgery | SARS-CoV-$2^+$ $HIV^+$ | SARS-CoV-$2^+$ $HIV^-$ | SARS-CoV-$2^-$ $HIV^+$ | SARS-CoV-$2^-$ $HIV^-$ |
|---|---|---|---|---|
| Placental localization | Attached to the fundus of the uterus and right adnexa | Left adnexa and left upper quadrant | Superior to the uterus, left paracolic and left adnexa | Attached to right broad ligament and adnexa of uterus |
| Placental vascular supply | Right infundibular pelvic vessels | Mesentery of the transverse colon, left infundibular pelvic and retroperitoneal vessels in the region of the aorta | Left infundibular pelivic artery | Right infundibular pelivic artery |
| Placental weight (grams) | 811 | 677 | Not available | Not available |

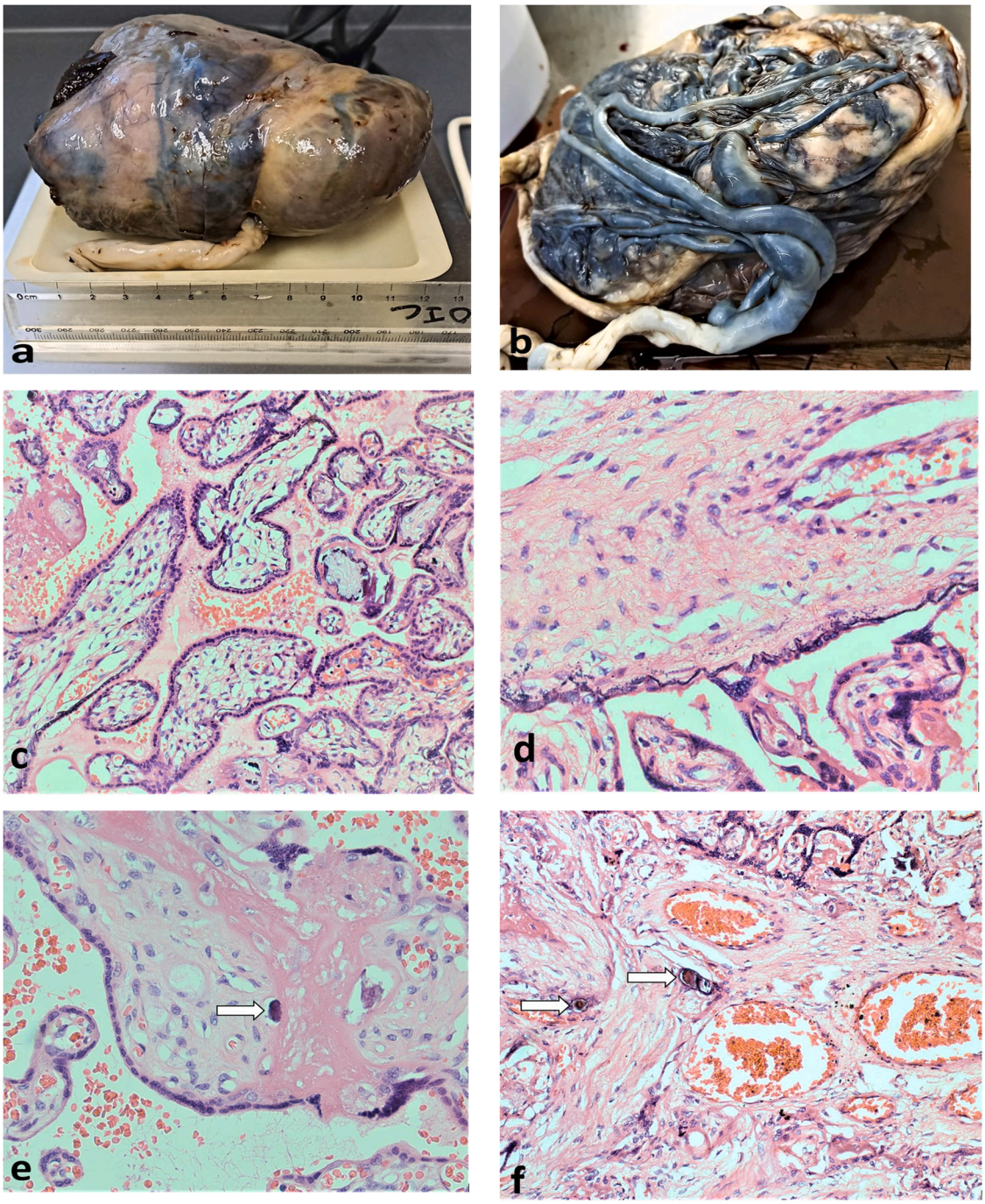


**Fig. 1.** Advanced abdominal pregnancy: Macroscopic lateral view of (a) SARS-CoV-2$^{+}$HIV$^{+}$ and (b) superior view of SARS-CoV-2$^{+}$HIV$^{-}$ placentae. Histopathological features of AAP SARS-CoV-2$^{+}$HIV$^{+}$ infected placental villi showing (c-d) mineralization of the basement membrane and (e-f) microcalcification (x40).

*Histopathological features*

The histopathological characteristics of all four AAPs are shown in Table 3. Foetal membranes for all placentae consisted of simple cuboidal epithelium resting on a thin basement membrane with underlying thin band of loose connective tissue. Dystrophic calcifications were observed in the decidua, septa and basal plate. Structurally, placental villi lying within the intervillous space were covered by a syncytiotrophoblast layer regardless of the infection type. The syncytiotrophoblast layer was made up of a multinucleated syncytium with eosinophilic cytoplasm, multiple intracytoplasmic vacuoles and pyknotic nuclei. Diffused multifocal syncytial knots were present in all placentae.

Mineralization of the basement membrane was noted in the HIV positive placenta regardless of SARS-CoV-2 infection (Fig. 1c-d). Syncytial degeneration/necrosis was also evident in all placentae, albeit amplified in the SARS-CoV-2 infected placenta (Fig. 1d-e). Villous microcalcifications (Fig. 1e-f) were noted in the SARS-CoV-2$^{+}$ HIV$^{+}$; SARS-CoV-2$^{+}$ HIV$^{-}$ and SARS-CoV-2$^{-}$ HIV$^{+}$ groups, being predominant in the COVID$^{+}$ infected placentae. Villitis and mononuclear inflammatory cells infiltrates (Fig. 2a) was noted in SARS-CoV-2$^{+}$ HIV$^{+}$, SARS-CoV-2$^{+}$HIV$^{-}$ and SARS-CoV-2$^{-}$HIV$^{+}$ placentae. Intravillous and perivillous fibrin deposition (Fig. 2b) was diffuse and widespread. Fibrin deposition was both focal and diffuse, occasionally with the avascular core being surrounded by a degenerative, irregular, syncytial trophoblast layer. Distal villous hypoplasia/mesenchymal dysplasia and patchy oedematous villi was also noted (Fig. 2c). Anuclear thinned-out syncytium

**Table 3**
Histopathological evaluation of the placenta.

| Histopathologic features | SARS-CoV-2$^{+}$ HIV$^{+}$ | SARS-CoV-2$^{+}$ HIV$^{-}$ | SARS-CoV-2$^{-}$ HIV$^{+}$ | SARS-CoV-2$^{-}$ HIV$^{-}$ |
|---|---|---|---|---|
| Mineralization of basement membrane | + + | + | + | – |
| Syncytial knots | + ++ | + ++ | + | + |
| Syncytial degeneration | + + | + + | + | + |
| Intravillous fibrin deposition | + ++ | + + | + | + |
| Perivillous fibrin deposition | + ++ | + + | + | + |
| Villous villitis (PBMCs) | + + | + | + | – |
| Thrombi | + + | + + | + | + |
| Ectasis | + + | + + | + | + |
| Mural hypertrophy | + + | + | + | – |
| Atherothic vessels | + + | + | + | – |
| Dystrophic microcalcification | + + | + + | + | – |

- nil effects seen; + liitle effects; + +moderate effects; + +significant effects; SARS-CoV-2$^{+}$:Covid positive; SARS-CoV-2$^{-}$:Covid negative; HIV +ve: HIV positive; HIV-ve: HIV negative

bulging over stromal capillaries into the intervillous space was also evident. High grade spatial and temporal foetal malperfusion was noted in SARS-CoV-2$^{+}$HIV$^{+}$; SARS-CoV-2 $^{+}$HIV$^{-}$ and SARS-CoV-2$^{-}$ HIV$^{+}$ placentae. These features included thrombi (Fig. 2d), ectasis (Fig. 2e-f), mural hypertrophy and atherotic vessels.

## Discussion

The main findings of this study were increased villitis, syncytiotrophoblast injury, mineralisation of synctiotrophoblast basement membrane, fibrin deposition, microcalcifications, vascular maladaptation and placental weight gain in the SARS-CoV-2$^{+}$ HIV$^{+}$ compared to SARS-CoV-2$^{+}$HIV$^{-}$ and SARS-CoV-2$^{-}$HIV$^{+}$ placentae.

### *Villitis*

We report inter- and intra-villous inflammation in placentae with SARS-CoV-2 and HIV infection and in a combination of both. Notably, SARS-CoV-2 infection causes chronic histiocytic intervillitis together with syncytiotrophoblast necrosis (15). The villitis may be an accrual of mononuclear inflammatory cells as previously reported [11]. These monocytoid cells express CD11c, CD14, CD68, and CD163, with some expressing myeloperoxidase+ CD66b+ neutrophils+ , a CD10- immature subgroup [12]. Notably, intervillitis has also been observed in Zika [13,14] and Dengue viral infections [15]. [[16]]. Villitis within the stroma is indicative of proinflammatory cytokine release, that induces vascular smooth muscle cells apoptosis. Moreover, SARS-CoV-2 related placental inflammation is believed to emanate from elevated IL-6 and TNF-α levels and is associated with endothelial dysfunction, thereby prompting maternal thromboembolic events [17]. We also observed thrombi in all the AAP placentae, being more pronounced in the SARS-CoV-2$^{+}$ placentae. Occlusive and non-occlusive thrombi have been previously graded by a working group in Amsterdam, highlighting the need for delineating diagnostic placental pathology values [18].

### *Synctiotrophoblast necrosis*

Apart from the maintenance of immune tolerance to fetal cells, syncytiotrophoblasts also serve as an immunological barrier against pathogens. In fact they are reported to sense viral pathogens via toll-like receptors and retinoic acid-inducible gene I-like receptors thereby mediating signal induction of type I interferons [19]. More recently, syncytiotrophoblast stress has been reported to include parvovirus infection albeit minimally, hence it is plausible that both HIV and SARS-CoV-2 infection would also aggravate the stress [20]. Notably, the denuding of the syncytiotrophoblast in our study may permit vertical transplacental foetal transmission of maternal SARS-CoV-2 infection since angiotensin-converting enzyme 2 (ACE2) and transmembrane protease serine 2 receptors (TMPRSS2) are expressed on its plasmalemma [21]. Also the syncytiotrophoblast necrosis observed in our study will influence the binding of SARS-CoV-2 to its ACE-2 and TMPRSS2 receptors on its plasmalemma [21].

### *Mineralisation of Synctiotrophoblast basement membrane*

We report pronounced mineralization of the syncytiotrophoblast basement membrane in the SARS-CoV-2$^{+}$HIV$^{+}$, SARS-CoV-2$^{+}$HIV$^{-}$ and SARS-CoV-2$^{-}$HIV$^{+}$, indicative of a general viral insult. Sedimentation of minerals, specifically calcium phosphate and haemosiderin on the syncytial basement membrane is related with fibrotic avascular villi [22]. Placental hemosiderin deposition was also previously observed in cytomegalovirus infection [31]. Mineralization of the syncytial basement membrane is associated with foetal vascular malperfusion and correlates with adverse foetal outcomes such as polyhydramnious, placental and fetal hydrops [23].

### *Fibrin deposition*

In our study, extensive fibrin deposition occurred in all placentae, being more prominent in the SARS-Co-V-2$^{+}$ placentae. Our findings are corroborated by others [16,24]. This pervasive fibrin deposition may be linked to placental malperfusion and poor fetal outcomes [25,26], corroborating the viable yet small-for-gestational-age neonates observed in our study. Nonetheless, in alveoli of acute respiratory distress syndrome (ARDS) in SARS-CoV-2 infections there is an accumulation of proteinaceous and fibrin exudate and macrophages [27]. Placental derived mesenchymal stem cells is believed to enhance the immunomodulatory and anti-inflammatory milieu of ARDS [27].

### *Microcalcifications*

We also report an increased prevalence of microcalcifications in the SARS-CoV-2$^{+}$ AAP placentae as corroborated by others [28]. These calcifications may emanate from syncytial trophoblast damage, or it may reflect a hypercoagulable state caused by SARS-Co-V-2 infection. Apoptotic bodies thereafter undergo osteogenic differentiation as they concentrate calcium and phosphate to allow crystal nucleation and mineralization [29]. Calcification of the placenta increases with gestational age, and may be associated with decreased placental perfusion, infarcts, still births and viral infections [30]. Notably these vascular calcifications represent a multifaceted connection of regulatory pathways such as adenosine signaling, osteochondrogenesis, inflammation, hypoxia, autophagy and phosphate signaling [31,32].

### *Vascular pathology*

Our findings demonstrate higher levels of vascular malperfusion in the SARS-CoV-2 positive AAP placentae, regardless of HIV status compared to the SARS-CoV-2 negative placentae. COVID-19-infected placentae are associated with aberrant vascular supply [12,33], and supports malperfusion features of mural hypertrophy, ectasis, atherosis and thrombi observed in our study. Maternal vascular malperfusion anomalies lead to fetoplacental underperfusion as observed in pre-eclampsia and hypercoagulable states such as antiphospholipid antibodies, lupus anticoagulant, factor V Leiden mutation, protein S and C deficiency [34]. Off note, placental hypoperfusion leads to maternal hypoxia following severe COVID-19 infection. Maternal vascular malperfusion features are more frequent in HIV infected (24.2%) compared to HIV uninfected women (12.6%) [35]. This pathology is associated with the development of hypertensive disorders of pregnancy and is

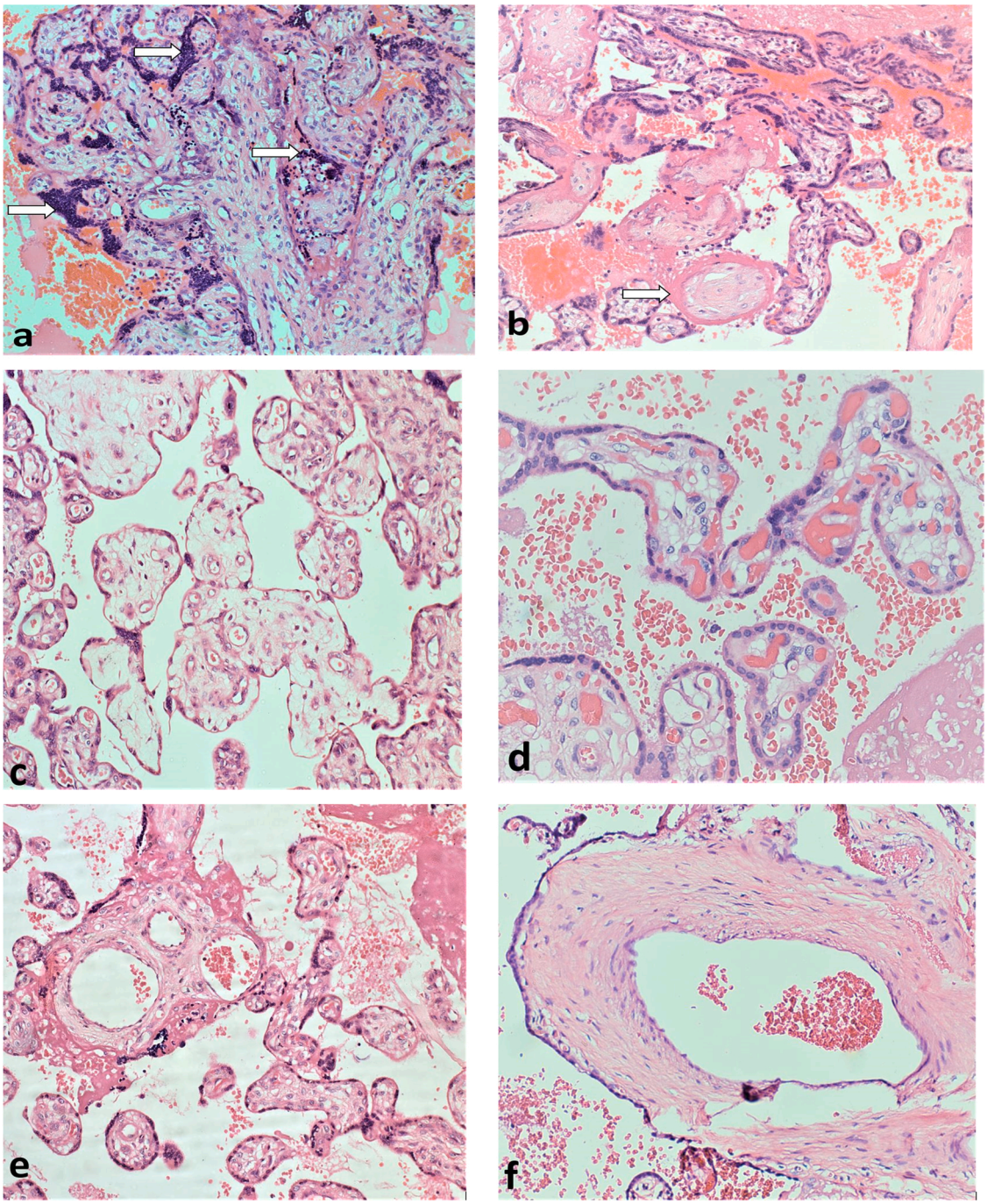


**Fig. 2.** Pathological features of SARS-CoV-2$^{+}$HIV$^{+}$ infected AAP placental villi showing (a) PBMC infiltration; (b) perivillous and intravillous fibrin; (c) mesenchymal dysplasia; (d) thrombi and (e-f) vascular ectasis (x40).

elevated in HIV-infected women receiving highly active antiretroviral therapy (HAART) [36,37]. Vascular malperfusion is also elevated in women on zidovudine (AZT) as observed in 76.47% out of 51 placentae of HIV positive mothers or nevirapine (NVP) compared to untreated cases [35]. Notably all HIV infected women in our study received anti-retroviral therapy, a standard of care in South Africa.

*Placental weight*

In our study, the SARS-CoV-2$^{+}$HIV$^{+}$ AAP placenta was almost twice the weight of a previously reported intrauterine SARS-CoV-2 infected placenta [38]. Tasca et al., (2021) reported heavier placental weight in COVID positive women receiving antibiotics or antivirals such as chloroquine [38]. It is plausible that SARS-CoV-2/HIV infection in pregnancy directly affects placental growth via viral infection, or indirectly through an exaggerated inflammatory response of the microenvironment. It is also possible that the gross increase in placental size may also be a compensatory proliferation of vascular supply to meet the increased oxygen and nutrient demands of the foetus required to support a viable neonate. Consistent with our findings, placental weight dysregulation [39,40], villitis, enhanced chorionitis/chorioamnionitis, funisitis membrane inflammation and vasculo-pathology have been reported in HIV infection [41].

*Foetal outcomes*

Nonetheless, we report good maternal and viable foetal outcomes in the third trimester of both SARS-CoV-2 infected AAPs regardless of their HIV status, indicating that close monitoring and appropriate patient management may avert termination of pregnancy, and prevent adverse maternal and poor foetal outcomes. However, one baby from the SARS-CoV-2$^{+}$HIV$^{+}$ AAP in our study was afflicted with dysmorphic facial features and a left foot deformity. This may be a consequence of low amniotic fluid volume and the absence of a "cushion effect". Notably, AAPs are associated with a high percentage (21%) of birth defects, limb and joint defects, facial and cranial asymmetry and deformity due to foetal compression [42].

*Treatment*

There is no standardization of treatment principles for AAP and peri-operative treatment options, which would improve newborn survival, and reduce maternal and neonatal morbidity. The diagnosis of AAP therefore creates a conundrum regarding clinical management as most cases are identified after 20 weeks with a live foetus. Decisions made regarding expectant management or immediate laparotomy are taken by both the patient and the attending clinician. Expectant management includes the patient being hospitalized for weeks under close observation because intra-abdominal bleeding cannot be predicted and may occur rapidly. A limitation of our study was the lack of a comparative group of intrauterine pregnancies; these should be investigated in future studies.

## Conclusion

This study highlights placental pathology of AAP pregnancies co-morbid with SARS-CoV-2 and HIV-1 viral insult. Pathological features include increased mineralisation of the syncytial basement membrane, microcalcifications, and villitis together with evidence of vascular adaptation in the SARS-CoV-2 compared to HIV-1 viral transgression alone. The characteristic of vascular maladaptation such as ectasis and mural hypertrophy indicate a compensatory response to meet the perils of a hypoxic insult of an AAP stemming from a need to meet the oxygen and nutrient demands of the foetus. Notably the pathological features of vascular malperfusion also occur in HIV infected women receiving antiretroviral therapy albeit at a lesser extent. Careful monitoring with suitable patient management will prevent early termination of AAPs co-infected with SARS-CoV-2 and HIV-1, thereby preserving maternal and foetal outcomes.

## Funding

This study was funded by productivity funds of Prof T Naicker.

## CRediT authorship contribution statement

**Dr S Ramphal**: Conceptualisation, design, critical revision of scientific content and approval of final version of manuscript. **Professor T Naicker**: Design, interpretation of data, writing and editing of manuscript, and approval of final version of manuscript. **Dr N Govender**: Design, interpretation of data, writing, editing and approval of final version of manuscript. **Mrs S Singh**: Analysis, interpretation of data, editing and approval of final version of manuscript. **Dr OP Khaliq**: Analysis, editing and approval of final version of manuscript.

## Declaration of Competing Interest

All Authors declare that there are no conflicts of interest.

## Acknowledgement

The authors wish to thank Professor Jagidesa Moodley for his expert advice and support in the conceptualization and design of the study.

## References

[1] Allinder SM, Fleischman J. The World's largest hiv epidemic in crisis: HIV in South Africa. CSIS Commentary; 2019.
[2] Clouse K, Malope-Kgokong B, Bor J, Nattey C, Mudau M, Maskew M. The South African National HIV pregnancy cohort: evaluating continuity of care among women living with HIV. BMC public health 2020;20(1):1–11.
[3] Thomson KA, Hughes J, Baeten JM, John-Stewart G, Celum C, Cohen CR, et al. Partners in prevention HSV/HIV transmission study and partners PrEP study teams, increased risk of HIV acquisition among women throughout pregnancy and during the postpartum period: a prospective per-coital-act analysis among women with HIV-infected partners. J Infect Dis 2018;218(1):16–25.
[4] Pattinson R, S Fawcus S, Gebhardt S, Soma-Pillay PN, PR, Moodley J. The impact of Covid-19 on use of maternal and reproductive health services and maternal and perinatal mortality. South African Health Review. In Press.
[5] Villar J, Ariff S, Gunier RB, Thiruvengadam R, Rauch S, Kholin A, et al. Maternal and neonatal morbidity and mortality among pregnant women with and without COVID-19 infection: the INTERCOVID multinational cohort study. JAMA Pediatr 2021;175(8):817–26.
[6] Worley KC, Hnat MD, Cunningham FG. Advanced extrauterine pregnancy: diagnostic and therapeutic challenges. Am J Obstet Gynecol 2008;198(3):e1–7. 297.
[7] Tolefac PN, Abanda MH, Minkande JZ, Priso EB. The challenge in the diagnosis and management of an advanced abdominal pregnancy in a resource-low setting: a case report. J Med Case Rep 2017;11(1):1–5.
[8] Ramphal S, Khaliq OP, Moodley J. Advanced Extra-uterine Pregnancy: A Review of the Literature. South African Journal of Obstetrics and Gynaecology. In Press.
[9] Burton G, Sebire N, Myatt L, Tannetta D, Wang Y-L, Sadovsky Y, et al. Optimising sample collection for placental research. Placenta 2014;35(1):9–22.
[10] Fischer AH, Jacobson KA, Rose J, Zeller R. Hematoxylin and eosin staining of tissue and cell sections. Cold Spring Harbor Prot 2008;2008(5). pdb. prot4986.
[11] Bos M, Nikkels PG, Cohen D, Schoones JW, Bloemenkamp KW, Bruijn JA, et al. Towards standardized criteria for diagnosing chronic intervillositis of unknown etiology: a systematic review. Placenta 2018;61:80–8.
[12] Facchetti F, Bugatti M, Drera E, Tripodo C, Sartori E, Cancila V, et al. SARS-CoV2 vertical transmission with adverse effects on the newborn revealed through integrated immunohistochemical, electron microscopy and molecular analyses of Placenta. EBioMedicine 2020;59:102951.
[13] Martines R, Bhatnagar J, Keating M, et al. Notes from the field: evidence of Zika virus infection in brain and placental tissues from two congenitally infected newborns and two fetal losses–Brazil, 2015. MMWR Morb Mortal Wkly Rep 2016; 65:159–60.
[14] Martines RB, Bhatnagar J, de Oliveira Ramos AM, Davi HPF, Iglezias SDA, Kanamura CT, et al. Pathology of congenital Zika syndrome in Brazil: a case series. Lancet 2016;388(10047):898–904.
[15] Ribeiro CF, Silami VG, Brasil P, Nogueira RMR. ickle-cell erythrocytes in the placentas of dengue-infected women. Int J Infect Dis 2012;16(1):e72.
[16] Schwartz DA, Baldewijns M, Benachi A, Bugatti M, Collins RR, De Luca D, et al. Chronic histiocytic intervillositis with trophoblast necrosis is a risk factor associated with placental infection from coronavirus disease 2019 (COVID-19) and intrauterine maternal-fetal severe acute respiratory syndrome coronavirus 2 (SARS-CoV-2) transmission in live-born and stillborn infants. Arch Pathol Lab Med 2021;145(5):517–28.
[17] Hosier H, Farhadian SF, Morotti RA, Deshmukh U, Lu-Culligan A, Campbell KH, et al. SARS–CoV-2 infection of the placenta. J Clin Investig 2020;130:9.
[18] Khong TY, Mooney EE, Ariel I, Balmus NC, Boyd TK, Brundler M-A, et al. Sampling and definitions of placental lesions: Amsterdam placental workshop group consensus statement. Arch Pathol Lab Med 2016;140(7):698–713.
[19] Rehwinkel J, Gack MU. RIG-I-like receptors: their regulation and roles in RNA sensing. Nat Rev Immunol 2020;20(9):537–51.
[20] Redman CW, Staff AC, Roberts JM. Syncytiotrophoblast stress in preeclampsia: the convergence point for multiple pathways. Am J Obstet Gynecol 2021.
[21] Taglauer E, Benarroch Y, Rop K, Barnett E, Sabharwal V, Yarrington C, et al. Consistent localization of SARS-CoV-2 spike glycoprotein and ACE2 over TMPRSS2 predominance in placental villi of 15 COVID-19 positive maternal-fetal dyads. Placenta 2020;100:69–74.
[22] Ariel I, Meir K. Mineralization of trophoblast basement membrane. Cham: Springer; 2019.
[23] Sebire NJ, Sepulveda W. Correlation of placental pathology with prenatal ultrasound findings. J Clin Pathol 2008;61(12):1276–84.
[24] Weber MA, Nikkels PG, Hamoen K, Duvekot JJ, De Krijger RR. Co-occurrence of massive perivillous fibrin deposition and chronic intervillositis: case report. Pediatr Dev Pathol 2006;9(3):234–8.
[25] Spinillo A, Gardella B, Muscettola G, Cesari S, Fiandrino G, Tzialla C. The impact of placental massive perivillous fibrin deposition on neonatal outcome in pregnancies complicated by fetal growth restriction. Placenta 2019;87:46–52.
[26] Mattuizzi A, Sauvestre F, André G, Poingt M, Camberlein C, Carles D, et al. Adverse perinatal outcomes of chronic intervillositis of unknown etiology: an observational retrospective study of 122 cases. Sci Rep 2020;10(1):1–9.

[27] Siddesh SE, Gowda DM, Jain R, Gulati A, Patil GS, Anudeep TC, et al. Placenta-derived mesenchymal stem cells (P-MSCs) for COVID-19 pneumonia—a regenerative dogma. Stem Cell Investig 2021:8.
[28] Singh N, Buckley T, Shertz W. Placental pathology in COVID-19: case series in a community hospital setting. Cureus. 2021;13:1.
[29] Shanahan CM. Inflammation ushers in calcification: a cycle of damage and protection?: Am Heart Assoc; 2007.
[30] Chitlange S, Hazari K, Joshi J, Shah R. AC M. Ultrasonographically observed preterm grade III placenta and perinatal outcome. Int J Gynaecol Obstet 1990;31 (4):325–8. Apr;. 1990.
[31] Hortells L, Sur St S, Hilaire C. Cell phenotype transitions in cardiovascular calcification. Front Cardiovasc Med 2018;5:27.
[32] Zazzeroni L, Faggioli G, Pasquinelli G. Mechanisms of arterial calcification: the role of matrix vesicles. Eur J Vasc Endovasc Surg 2018;55:425–32.
[33] Ferraiolo A, Barra F, Kratochwila C, Paudice M, Vellone VG, Godano E, et al. Report of positive placental swabs for SARS-CoV-2 in an asymptomatic pregnant woman with COVID-19. Medicina 2020;56(6):306.
[34] Manco-Johnson MJ, Abshire TC, Jacobson LJ, Marlar RA. Severe neonatal protein C deficiency: prevalence and thrombotic risk. J. Pediatr 1991;119(5):793–8.
[35] Kalk E, Schubert P, Bettinger JA, Cotton MF, Esser M, Slogrove A, et al. Placental pathology in HIV infection at term: a comparison with HIV-uninfected women. Trop Med Int Health 2017;22(5):604–13.
[36] Papp E., Loutfy M., Yudin M., editors. Angiogenesis and Adverse Pregnancy Outcomes in Women with HIV: the AAPH study. 3rd International Workshop on HIV & Women; 2013.
[37] Shapiro RL, Souda S, Parekh N, Binda K, Kayembe M, Lockman S, et al. High prevalence of hypertension and placental insufficiency, but no in utero HIV transmission, among women on HAART with stillbirths in Botswana. PLoS One 2012;7(2):e31580.
[38] Tasca C, Rossi RS, Corti S, Anelli GM, Savasi V, Brunetti F, et al. Placental pathology in COVID-19 affected pregnant women: a prospective case-control study. Placenta 2021;110:9–15.
[39] Jauniaux E, Nessmann C, Imbert MC, Meuris S, Puissant F, Hustin J. Morphological aspects of the placenta in HIV pregnancies. Placenta 1988;9(6):633–42.
[40] Gichangi PB, Nyongo A, Temmerman M. Pregnancy outcome and placental weights: their relationship to HIV-1 infection. East Afr Med J 1993;70(2):85–9.
[41] Backé E, Jimenez E, Unger M, Schäfer A, Vocks-Hauck M, Grosch-Wörner I, et al. Vertical human immunodeficiency virus transmission: a study of placental pathology in relation to maternal risk factors. Am J Perinatol 1994;11(05):326–30.
[42] Stevens CA. Malformations and deformations in abdominal pregnancy. Am J Med Genet 1993;47(8):1189–95.